REPORT DOCUMENTATION PAGE

Form Approved
OMB No. 0704-0188

1. REPORT DATE *(DD-MM-YYYY)*	2. REPORT TYPE	3. DATES COVERED *(From - To)*
14-03-2008	Final Report	07/01/2004 - 12/31/2007

4. TITLE AND SUBTITLE
3-5 μm Room Temperature Operated CW Laser Diodes Based on Novel InGaAsNSb Material System.

5a. CONTRACT NUMBER

5b. GRANT NUMBER
FA9550-04-1-0372

5c. PROGRAM ELEMENT NUMBER

6. AUTHOR(S)
Gregory Belenky

5d. PROJECT NUMBER

5e. TASK NUMBER

5f. WORK UNIT NUMBER

7. PERFORMING ORGANIZATION NAME(S) AND ADDRESS(ES)
State University of New York at Stony Brook

8. PERFORMING ORGANIZATION REPORT NUMBER

9. SPONSORING / MONITORING AGENCY NAME(S) AND ADDRESS(ES)
AFOSR
875 N Randolph St, Suite 325 Dr. Don Silversmith /NE
Room 3112
Arlington, VA 22203

10. SPONSOR/MONITOR'S ACRONYM(S)
AFOSR/NE

11. SPONSOR/MONITOR'S REPORT NUMBER(S)

12. DISTRIBUTION / AVAILABILITY STATEMENT

Distribution Statement A: Unlimited

AFRL-SR-AR-TR-08-0170

13. SUPPLEMENTARY NOTES

20080404107

14. ABSTRACT

Novel mid-IR photonic device technology has been developed. High power room temperature operated diode lasers for spectral region above 3μm have been designed and fabricated. 120mW CW output power level was obtained at 3μm and 80mW CW at 3.1μm at room temperature. More than 200mW CW output was obtained near 3μm at temperatures accessible with thermo-electric cooling.

We demonstrate a double-quantum-well GaSb-based diode laser operating at 2.3-2.4μm with a room-temperature CW output power above 1W and a maximum power-conversion efficiency of 17.5 %.

Insufficient hole confinement in GaSb-based photonic nanostructures reported prior to this project work was identified by set of specially designed experimental studies and by theoretical modeling. We have developed novel design approach based on combination of strain engineered active region and quinternary barrier material to fabricate watt class efficient diode lasers for spectral region from 3 to 3.5μm. These new devices will substitute bulky optically pumped solid-state light emitters with poor power conversion efficiency or cryogenically cooled semiconductor lasers in several important home security application.

15. SUBJECT TERMS

16. SECURITY CLASSIFICATION OF:			17. LIMITATION OF ABSTRACT	18. NUMBER OF PAGES	19a. NAME OF RESPONSIBLE PERSON
a. REPORT	b. ABSTRACT	c. THIS PAGE			19b. TELEPHONE NUMBER *(include area code)*

Project results

New class of continuous wave room temperature operated GaSb-based mid-infrared lasers and light emitting diodes was developed. High power diode lasers operating in spectral region from 3 to 3.5μm in continuous wave regime with hundred mW level of output power above 3μm at room temperature were designed and fabricated for the first time.

World record high power room temperature operated 2.3-2.4μm GaSb-based mid-infrared lasers were designed, grown, fabricated, packaged and characterized at Stony Brook University. Power conversion efficiency of 17.5% was achieved for single emitters operating in CW regime at room temperature.

New approach to design of the type-I QW GaSb-based high power room temperature operated was developed. Specific features and special importance of the heavy strain in InGaAsSb QWs were theoretically analyzed and included in novel GaSb-based mid-infrared photonic device design concept. Quinternary AlInGaAsSb barrier material was developed to assist hole localization in mid-infrared diode lasers active region leading to dramatic improvement of the lasers room temperature performance parameters.

Carrier capture in InAs/InGaAsSb electron QW, InGaSb/InGaAsSb hole QW and InAs/InGaSb/InGaAsSb W-QW was studied using photoluminescence up-conversion and temperature resolved photoluminescence. We report on direct observation of the pour hole capture in W-QWs that contributes to suppression of the corresponding laser performance at high temperatures.

1. Introduction.

Laser sources operating in spectral region 2 – 3.5 μm are in demand for ultra-sensitive laser spectroscopy, medical diagnostics, home security, industrial process monitoring, infrared countermeasures, optical wireless communications, etc. Currently, solid state lasers and optical parametric oscillators and amplifiers are used as coherent light sources in this spectral region. Solid state and parametric sources are being optically pumped by near infrared diode lasers. This intermediate energy transfer step from near infrared pumping diode to mid infrared emitting device reduces power-conversion system efficiency. Availability of the highly efficient semiconductor diode lasers operating in 2 – 3.5 μm spectral region will significantly improve the performance of the many existing systems and enable new applications.

In the framework of this project we have achieved major breakthrough in the development of the GaSb-based technology of high power room temperature operated mid-IR type-I QW diode lasers operating above 3μm. Room temperature CW operation was demonstrated for 3-3.4μm diode lasers. Stony Brook University has developed complete in-house GaSb-based photonic device fabrication technology based on acquired in year 2006 molecular beam epitaxy system (VEECO GEN-930) and class 100 clean room facilities recently supplemented by reactive ion etching and laser mirror coating systems.

Figure below shows the picture of the newly acquired GEN-930 solid source molecular beam epitaxy (MBE) system installed and operated at Stony Brook University and dedicated to GaSb-based photonic device development.

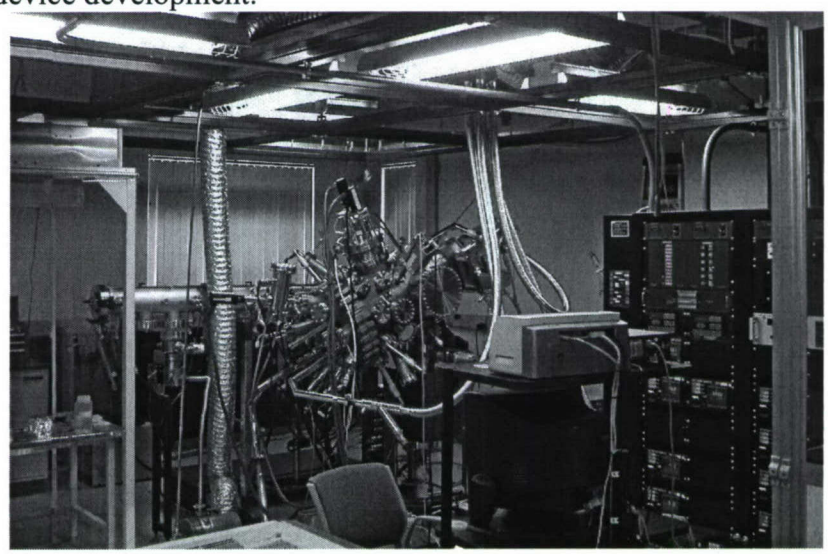

1. Compressively strained quantum wells for 2.3-2.4 micron wavelength range.

We have performed the detailed modeling and experimental studies of the laser structures characterized by different QW compositions and, correspondingly, different strain and different hole confinements.

Theoretical.

In GaInAsSb/AlGaAsSb quantum wells (QWs), the band offsets at the heterointerfaces are unevenly distributed between conduction and valence bands leading to excessive electron and deficient hole confinements. Since the electrons are strongly localized in deep conduction band QWs, the thermal redistribution of holes between the shallow valence band QWs and the optical waveguide layers creates Coulomb barriers which can improve the hole confinement to some

extent. Even in this case, however, the bulk heavy-hole states of the waveguide material with very high density of states (DOS) remain energetically close to the lasing states in the uppermost hole subband and, therefore, unfavorably affect the population of the lasing states. This situation can be improved by using the compressively strained QW layers which deepens the heavy-hole QWs and, therefore, enhances the population of the upper (lasing) hole subband and increases the structure optical gain.

It is well established fact that compressive strain in active QWs improves the laser differential gain by balancing the DOS in the joint lasing subbands. Compressive strain splits the first heavy-hole (HH) and first light-hole (LH) subbands and reduces the band-edge heavy-hole DOS, which otherwise is unfavorably increased by HH-LH subband mixing. This mechanism of gain improvement, however, works well only for compressive strain level up to 1%. Strain values beyond that range have little additional effect on the band-edge heavy-hole DOS, since at such a high strain the HH and LH subbands are already well separated in energy. We emphasize that, due to the inherently low valence band offsets at the quaternary GaInAsSb/AlGaAsSb interfaces, the QW compressive strain manifest itself not only through the band-edge HH DOS reduction but, mainly, by increasing the effective barrier height for the quantum-confined HH states. Compressive strain moves the position of the QW HH states upwards thus making the heavy-hole QW deeper. Improved HH confinement, in turn, reduces the thermally activated hole redistribution between the QW subbands and the adjoin bulk barrier states and, therefore, increases the occupation of the uppermost hole subband states participating in the lasing transition. This ultimately enhances the laser differential gain and reduces the threshold current density. Our calculations show that the enhancement of the optical gain in Sb-based lasers through the strain-induced increase of the HH confinement remains efficient for high compressive strains in the 1%-2% range while preserving the benefit of the balanced joint DOS achieved at the lower strain level.

Effect of the QW strain on the hole confinement becomes even more important in InGaAsSb/AlGaAsSb QW lasers when we move to longer emission wavelengths. In this case, more indium is needed in the QW composition which correspondingly requires higher QW arsenic concentration to avoid excessive strain build-up. Higher arsenic contents lowers the valence band position in the QW material and deteriorates the hole confinement. As a result, in QWs with indium concentration above 50%, which brings the laser emission above 3 μm, the QW compressive strain becomes completely responsible for the hole confinement in structures with 25% aluminum in the waveguide. As a result, to ensure the adequate hole confinement in the long-wavelength lasers, highly strained (up to 2%) QWs should be complemented by the waveguides with higher aluminum contents of about 35%.

We illustrate the effect of the strain on the laser performance by calculating the modal optical gain in structures with low (1%) and high (1.5%) level of compressive strain in the active QWs. According to our estimation, the hole confinement in the first structure was insufficient, with valence band QW depth for heavy holes of only 35 meV. The second structure was designed for the same lasing wavelength with lower QW arsenic concentration and higher compressive strain. Due to combination of composition and strain the confining barriers for heavy holes in this structure were increased to 105 meV. Calculations show that this improvement of the hole confinement is primarily responsible for the observed enhancement of the optical gain, while the strain-induced subband DOS balancing was of secondary importance. Our calculations are based on the 8-band model of the electron energy spectrum in cubic semiconductors including strain-induced modifications of band positions in the compressively strained QWs. The resulting 8-

band Schrödinger equation was solved self-consistently with the Poisson equation using the COMSOL software. During each iteration, the hole populations and Fermi distribution functions in each hole subband were recalculated taking into account thermal redistribution of holes between QW and waveguide. The iteration cycle was repeated until quasi-Fermi level position in valence band was stabilized and conversions was reached, which took 5-10 iterations depending on the injected hole concentration and carrier temperature. In modeled structures, electrons were strongly localized in conduction-band QWs, occupying predominantly the lowest electronic subband.

Figure 1.1 illustrates our choice of material compositions for strained QW structures with enhanced hole confinement. Data for binary materials and ternary alloys used in these calculations were taken from review by I. Vurgaftman et al, J. Appl. Phys. 89, 5815 (2001). The quaternary alloy band gaps were calculated using biquadratic interpolation algorithm. Figure 1.1a shows the arsenic vs. indium concentration dependencies for iso-strain QW compositions. The compositions with indium contents above 30% are of major interest for the QW MIR-lasers. Figures 1.1b and 1.1c show the calculated energy gaps and heavy-hole band edge positions in quaternary GaInAsSb compositions with different values of compressive strain. It is readily seen that highly strained indium-rich QW compositions benefit from improved hole confinement while retaining sufficiently low values of the optical gap.

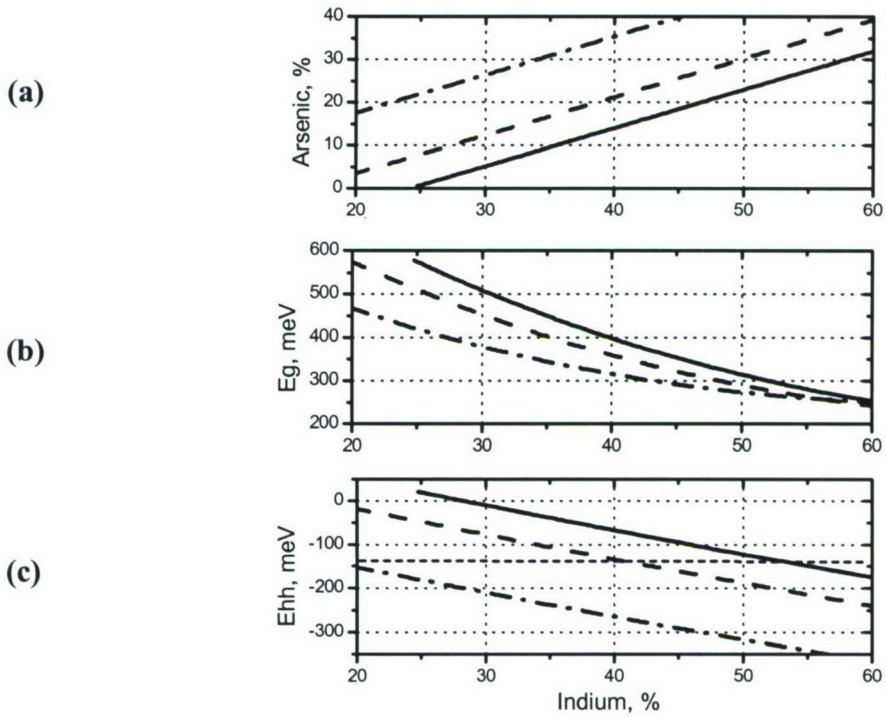

Figure 1.1. Isostrain lines in quaternary GaInAsSb alloy system: dash-doted lines - alloy composition lattice matched to GaSb, dashed lines – composition with 1.0 % compressive strain, solid lines - 1.5 % compressive strain. **a)** Arsenic vs. indium concentration in GaInAsSb alloys. **b)** Fundamental energy gap in GaInAsSb alloys with different strains. **c)** Strain-induced modification of the heavy-hole band edge position. Horizontal dashed line indicates the positions of the valence band edge in the barrier AlGaAsSb alloys with 25% aluminum concentrations.

Figure 1.2 illustrates the process of strain-induced balancing of electron and hole DOS in GaSb-based QW heterostructures.

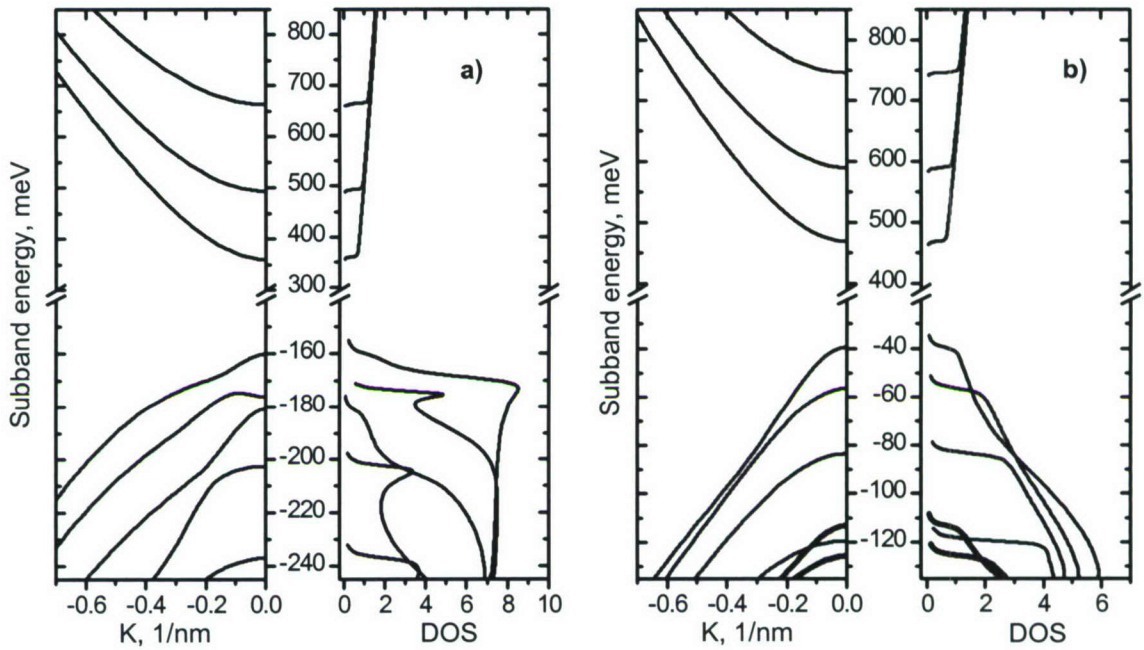

Figure 1.2. Strain-induced balancing of electron and hole DOS: **(a)** Lattice matched $Al_{0.5}Ga_{0.5}As_{0.04}Sb_{0.96}/Ga_{0.8}In_{0.2}As_{0.2}Sb_{0.8}$ QW heterostructure; **(b)** Strained $Al_{0.25}Ga_{0.75}As_{0.02}Sb_{0.98}/Ga_{0.65}In_{0.35}As_{0.09}Sb_{0.91}$ QW heterostructure with compressively strained QW (strain 1.5%). Left panel of each plot shows the subband dispersion, *i.e.* the subband energy *vs.* the electron/hole wavevector K; right panel shows the subband DOS (in 10^{10}/meV*cm^2). Note the difference in energy scale for valence band subbands in figures **(a)** and **(b)**. Two bold lines in the lower part of each panel of figure **(b)** show valence subbands and DOS for QW composition $Ga_{0.65}In_{0.35}As_{0.17}Sb_{0.83}$ with 1% strain.

Figure 1.2a shows energy subbands (left panel) and subband DOS (right panel) in an exemplary lattice matched (unstrained) $Al_{0.5}Ga_{0.5}As_{0.04}Sb_{0.96}/Ga_{0.8}In_{0.2}As_{0.2}Sb_{0.8}$ QW structure. Electron and hole subbands have noticeably different DOS in unstrained QW due to the anticrossing between second (heavy-hole) and third (light-hole) valence subbands, which induces strong subband nonparabolicity. Figure 1.2b demonstrates much better balance between lower electron and upper hole subband DOS in $Al_{0.25}Ga_{0.75}As_{0.02}Sb_{0.98}/Ga_{0.65}In_{0.35}As_{0.09}Sb_{0.91}$ heterostructure with highly compressively strained QW (strain 1.5%). All three upper hole subbands are now of heavy-hole type at $K = 0$ and no anticrossing effects are visible in the subband DOC structure. Bold lines in Figure 1.2b show the valence subbands and DOS for QW with higher arsenic concentration (17%) and lower strain (1%). According to our calculations, this structure is characterized by heavy-hole QW depth of only 35 meV. It is readily seen though that the DOS at the upper subband edge in this shallow QW does not differ noticeably from the DOS of the uppermost states in deeper QW of structure. The most striking difference between two structures is the hole confinement which is significantly lower in structure with lower strain. Large value of valence band DOS in bulk waveguide layers dominates the thermal hole redistribution in shallow QW and strongly reduces the population of the hole lasing states. Such

redistribution can noticeably deteriorate the optical gain in the laser structure. Figure 1.3 shows peak modal gain at three different temperatures calculated as a function of the injected carrier concentration for structures with low strain (1.0%, dashed curves) and high strain (1.5%, solid lines).

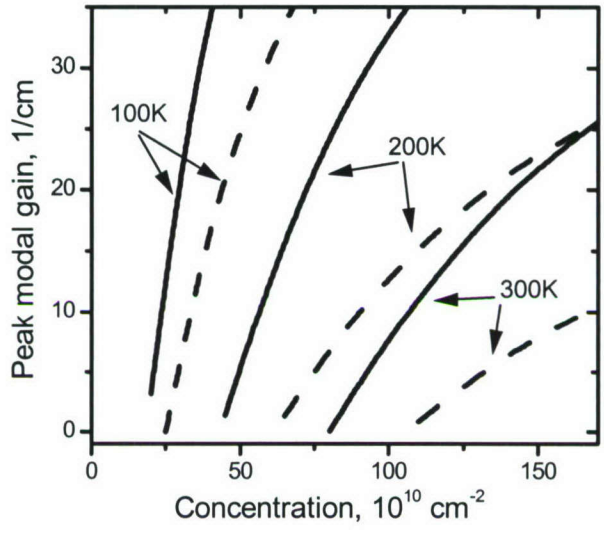

Figure 1.3. Peak modal gain as a function of the injected carrier concentration in QW for different temperatures. Dashed lines indicate structure with 1% compressive strain, solid lines – structure with 1.5% strain.

Strain-induced deepening of the HH QW reduces thermal redistribution of the holes between QW and waveguide and, for the same total carrier concentration, increases the occupation of the upper heavy-hole subband states participating in lasing transition. The implication of the improved hole confinement for optical gain is straightforward – structure with better hole confinement demonstrates higher differential gain and lower threshold concentration; see Figure 1.3. Due to large conduction band offsets in the In(Al)GaAsSb system the effect of thermal electron redistribution into the higher electron subbands and electron continuum was negligible. The resulting difference in electron and hole spatial distributions creates band bending which to some extent improves the hole confinement in shallow hole QW of structure. This effect was taken into account self-consistently in our gain calculations.

Concluding this theoretical introduction, we emphasize the importance of the QW strain engineering in type-I QW GaSb-based lasers. Specific feature of the GaIn(Al)AsSb material system is relatively low valence band offsets between optically active QWs and waveguide (barrier) layers. The hole confinement can be significantly improved by use of the heavily compressively strained GaInAsSb QWs. In contrast to strain-induced DOS balancing, which is efficient for strain values up to 1%, this mechanism remains efficient in GaSb-based materials at higher compressive strain levels.

Experimental

In order to verify the theoretical predictions we have designed and fabricated two laser heterostructures emitting at 2.3μm. One sample employed two 10-μm-wide $In_{0.35}Ga_{0.65}As_{0.17}Sb_{0.83}$ quantum wells, which led to 1% compressive strain. The other sample had two 12-μm-wide $In_{0.35}Ga_{0.65}As_{0.09}Sb_{0.91}$ quantum wells, which leaded to 1.5% compressive strain. Except for the

difference above, the lasers have identical structure. The laser heterostructures were grown using a Veeco GEN-930 solid source molecular beam epitaxy system on Te-doped GaSb substrates. The cladding layers were 1.5μm wide $Al_{0.9}Ga_{0.1}As_{0.07}Sb_{0.93}$ doped with Te (n-side) and Be (p-side). Graded bandgap heavily doped transition layers were introduced between the substrate and n-cladding and between the p-cladding and p-cap to assist carrier injection. The nominally undoped $Al_{0.25}Ga_{0.75}As_{0.02}Sb_{0.98}$ waveguide layer with a total thickness of about 800nm contained two $In_{0.35}Ga_{0.63}As_ySb_{1-y}$ QWs centered in the waveguide and spaced 20nm apart. The thick waveguide and cladding layers were lattice matched to GaSb. The wafer was processed into 100μm-wide silicon nitride confined gain guided lasers. 1mm-long uncoated lasers were In-soldered epi-side up onto Au-coated polished copper blocks and characterized in short pulse mode (200ns/1MHz).

Figure1.4 shows that lower threshold current, 0.14A, and higher slope efficiency, 0.16 W/A, was achieved for lasers with 1.5% compressive strain compared threshold current, 0.24 A, and slope efficiency, 0.15 W/A, for lasers with 1% compressive strain at room temperature.

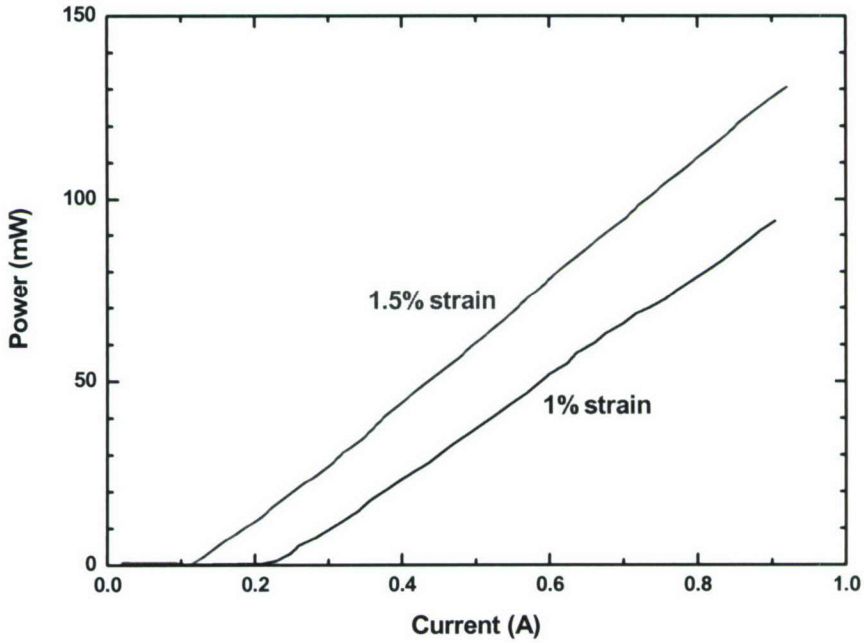

Figure 1.4. Pulsed light-current characteristics 1-mm uncoated lasers at the repetition rate of 1MHz and duration time of 200ns

Nearly twofold reduction of the threshold current with strain increase is explained by enhancement of the differential gain with respect to current (Figure 1.5). Figure 1.5 shows the peak modal gain as a function of under-threshold current as obtained from Hakki-Paoli measurements supplemented by a spatial filtering technique. A strong increase in differential gain is observed in the structure with higher active region compressive strain in accordance with modeling predictions. At 200K the difference between the rates of gain increase with current in lasers with 1% and 1.5% QW strains decreases since hole confinement barrier becomes adequate in both lasers at low temperatures.

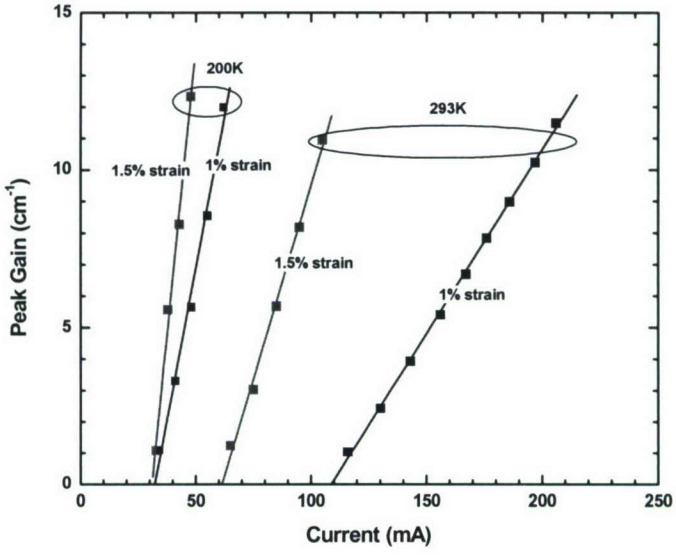

Figure 1.5. Differential gain for lasers with QW compressive strain 1.5% (red) 1% (blue) at 200K and at 293K.

Based on the aforementioned findings we have developed design and in-house technology of the 2.3-2.4 μm GaSb-based type-I QW laser with low threshold current. Figure 1.6 shows the room temperature continuous wave light-current-voltage characteristics of the 100μm-wide multimode diode lasers mounted epi-down on copper heatsink and emitting near 2.4μm. Both 1mm- and 2mm-long devices demonstrate world record performance giving 850mW and 1050mW at room temperature in continuous wave mode.

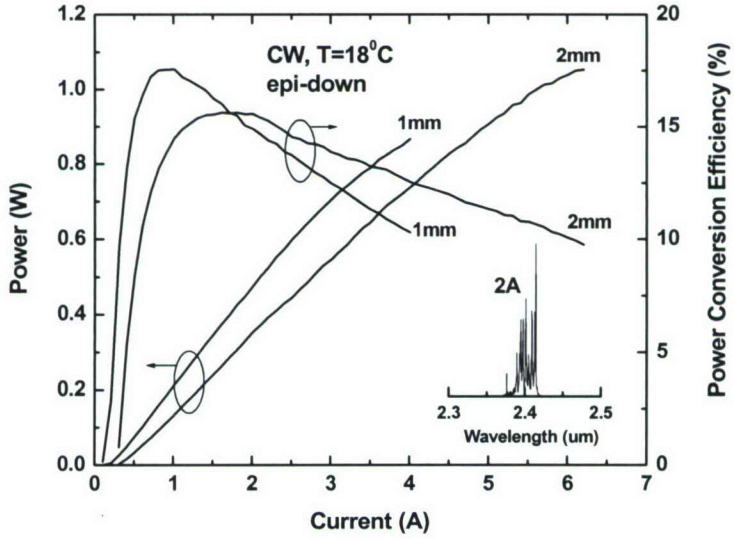

Figure 1.6. Light-current and power-conversion characteristics of the 2.4μm GaSb-based lasers.

Figure 1.7 (left) shows the room temperature continuous wave light-current and power-conversion characteristics of the 100μm-wide multimode diode lasers mounted epi-down on copper heatsink and emitting near 2.3μm. Both 1mm- and 2mm-long devices demonstrate world record performance giving 850mW and 1150mW at room temperature in continuous wave mode.

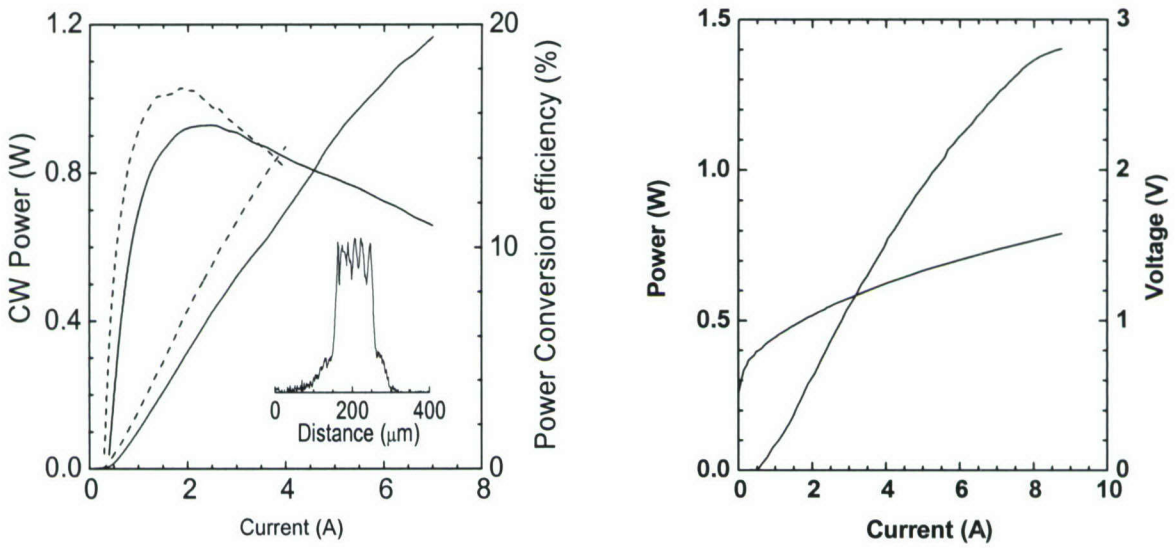

Figure 1.7. (left) CW Light-current-"power-conversion" characteristics of the 2.3μm lasers with 1mm-long (dashed) and 2mm-long (solid) cavity lengths. Insert shows lateral near field; (right) Quasi-CW power (measured under 30 μs pulse width, 300 Hz repetition rate) and voltage–current characteristics of 2-mm lasers obtained at the heatsink temperature of 18°C.

The devices have also been tested in the quasi-QW mode (Figure 1.7b) under the 30-μs-long current pulses with repetition frequency of 300. The maximum QCW power of 1.4 W was obtained at the current of 8.5 A. The voltage drop across the laser heterostructure was below 1.5 V up to the current value of 8 A leading to above 12% power conversion efficiency at 1W CW output. Maximum power conversion efficiency achieved for 2.3-2.4μm devices was 17.5% setting new world record in this spectral region.

2. High power diode lasers for spectral region above 3μm.

High-power room temperature operated semiconductor lasers operating in spectral region from 3 to 3.5μm are in demand for variety of applications including remote chemical and biologic agent spectral analysis, infrared illumination and countermeasures, medical diagnostics and treatment, etc. The task of development of the corresponding devices still poses significant challenge for any of contemporary approaches to mid-infrared semiconductor laser design. Insufficient conduction band offset prevents extension of high-power room temperature operation of intersubband quantum cascade devices in this spectral region. Novel technology of the InAs-based intersubband quantum cascade devices solves this problem but still device room temperature operation is limited to short pulse mode. Interband GaSb-based laser heterostructures in both cascade and diode arrangement demonstrate excellent electron confinement but might suffer from insufficient confinement of holes. Type-II GaSb-based interband quantum cascade lasers have recently demonstrated continuous-wave (CW) operation up to 260K temperature but with limited output power and at wavelength above 3.3μm. CW

operation was achieved for type-I quantum-well (QW) GaSb-based diode lasers with wavelength of 3.04μm and with output power below 5mW. We report on extension of the wavelength of CW high power room temperature operated type-I QW GaSb-based diode lasers with quaternary AlGaAsSb barrier up to 3.1μm together with significant improvement of their output power level.

It was argued that the rise of the Auger recombination rate should prevent extension of the room temperature CW operation wavelength of interband emitters. We have shown that it is degradation of the hole confinement barrier in the In-rich InGaAsSb/AlGaAsSb type-I QWs of GaSb-based laser heterostructures that contributes to excessive temperature sensitivity of the laser parameters. It was demonstrated that introduction of the heavy compressive strain into these QWs improves valence band offset leading to reduction threshold current density and its temperature sensitivity. These findings defined the design approach used for development of the 3.1μm diode lasers reported in this paper. Namely, to facilitate the QW hole confinement the Al content of the quaternary barrier material was increased up to 35% (as compared to 25% used for 2.4μm devices) and InGaAsSb QW compressive strain was increased up to 1.8%.

Laser heterostructures have been grown by solid-source molecular beam epitaxy using SUNY's Veeco GEN-930 reactor equipped with As and Sb valved cracker sources. Te and Be were used for n- and p-doping, respectively. Laser active region contained two 12nm-wide 100nm-spaced 1.8% compressively strained InGaAsSb QWs with nominal In composition of about 50%. Waveguide (total width of 1μm) and barrier material was $Al_{0.35}Ga_{0.65}As_{0.03}Sb_{0.97}$. Cladding material was $Al_{0.9}Ga_{0.1}As_{0.07}Sb_{0.93}$. Graded bandgap heavily doped transition layers were introduced between the substrate and n-cladding and between the p-cladding and GaSb p-cap to assist carrier injection. The wafer was processed into 100μm-wide silicon nitride confined gain guided lasers. Lasers were neutral-(NR~30%) and high-reflection (HR~95%) coated, In-soldered epi-side down onto Au-coated polished copper blocks, and mounted either onto closed cycle cryostat cold finger or onto water cooled copper block for characterization.

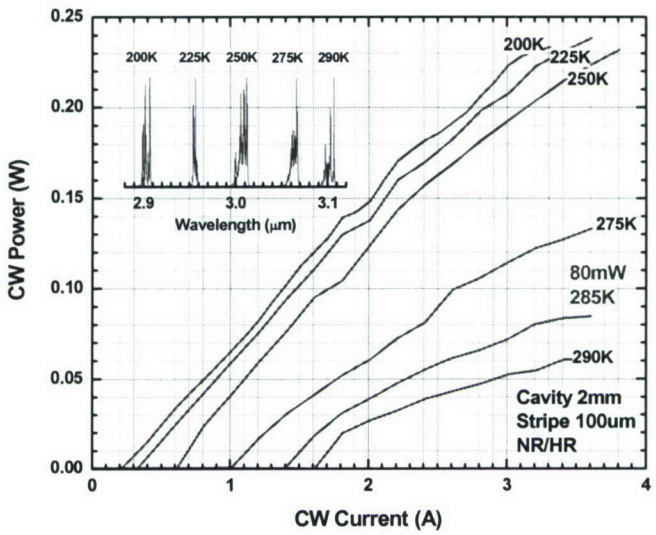

Figure 2.1. Temperature dependence of CW light-current characteristics of the GaSb-based lasers emitting at 3.1μm at room temperature. Insert shows laser spectra near threshold.

Figure 2.1 shows the temperature dependence of CW light-current characteristics for 2-mm-long lasers. Devices demonstrate threshold current density of 300A/cm^2 (150A/cm^2 per QW) and output power above 200mW CW at 250K (λ=3μm). With temperature increase the device CW threshold current density increases and reaches value of 800A/cm^2 (400A/cm^2 per QW) at 290K (λ=3.1μm). CW slope efficiency remains nearly unchanged in temperature range from 200 to 250K and decreases from 250 to 290K. Maximum CW output power was above 80mW at 12^{0}C limited by thermal roll-over at the current of 3.5A. Voltage drop across laser diode at the maximum output power level was below 1.5V at room temperature.

Figure 2.2 shows the short pulse light-current characteristics of the 2mm-long devices characterized at temperatures in the range from 200K to 350K. In short pulse mode (150ns/10kHz) peak output power reached above 750mW at room temperature at the current of 15A and device slope efficiency remained current independent up to 5A. At lower temperatures the device peak output power was above 1W.

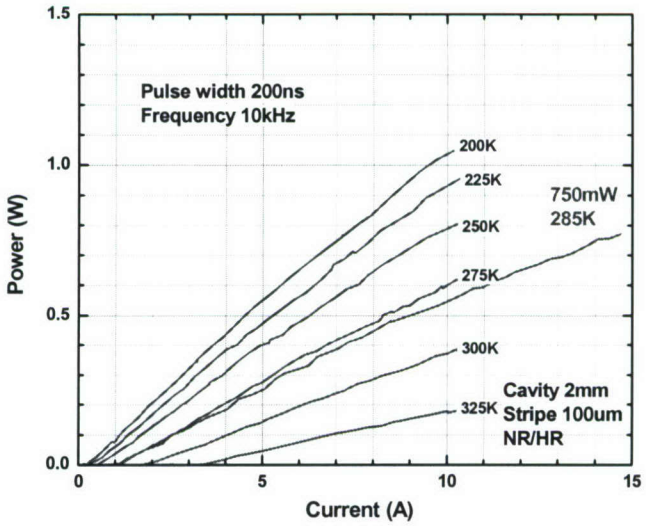

Figure 2.2. Temperature dependence of pulsed light-current characteristics of the GaSb-based lasers emitting at 3.1μm at room temperature.

The improved 3.1μm device output performance correlates with two laser heterostructure modifications both expected to improved hole confinement barrier, i.e. more Al in waveguide and high compressive strain in QWs. There were no special active region modifications done that are expected to modify Auger recombination coefficient. It was shown in that nonradiative, mainly, Auger recombination is responsible for up to 80% of the type-I QW GaSb-based diode laser threshold current even at 2.37μm. It was argued that dominance of the Auger process is responsible for strong temperature sensitivity of the laser threshold current density and, hence, should limit CW output power level. The prevailing mechanism of the Auger recombination in type-I GaSb-based diode lasers, most probably, is not associated with spin-orbit split (SO) band due to larger than bandgap estimated value of the spin-orbit band splitting even in devices lasing at 2.3μm. Another Auger processes, for instance, associated with electron transition upward in conduction band (CHCC) were suggested to explain nonradiative nature of the 80% of the threshold current in 2.37μm lasers. These Auger processes, if indeed present, should be enhanced substantially for 3.1μm lasers reported in this work. At the same time Figure 1 demonstrates

unambiguously the possibility of high power room temperature operation in this spectral region. We speculate that CW high power room temperature operation at 3.1μm was achieved by improvement of the QW hole confinement. Increase of the valence band discontinuity not only can improve laser efficiency and device differential gain with respect to concentration but also can minimize contribution of the CHCC Auger process by reducing threshold carrier concentration.

The plausible mechanism is described below. In interband GaSb-based diode lasers the confinement barriers for electrons are more than satisfactory (above 500meV). Electrons captured and confined in deep conduction band QWs create electrostatic band bending and confine holes in the vicinity of the QWs. This Coulomb attraction might, to some extend, compensate for lack of valence band offset and still provide for hole localization in the vicinity of electrons. However, threshold carrier concentration required to reach threshold gain is higher for the case of Coulomb assisted hole confinement as compared to the situation when hole confinement is achieved solely by satisfactory valence band discontinuity. Extra threshold concentration in former case comes from necessity to occupy a set of Coulomb confined subbands with inherently large density of states. Increase of the electron and hole threshold carrier concentration triggers Auger process which in turn can increase corresponding laser threshold current density and its temperature sensitivity.

Incorporation of indium into the waveguide results in increased arsenic concentration in order to provide lattice-matching to GaSb. These compositional changes lower the valence band energy in the barrier and, consequently, improve the hole confinement in the QW. In addition, the QW depth for electrons decreases favoring more homogenous QW population in multi-QW laser heterostructures. Figure 2.3 shows the valence and conduction band edge energies versus indium composition in the barrier calculated using biquadratic interpolation algorithm.

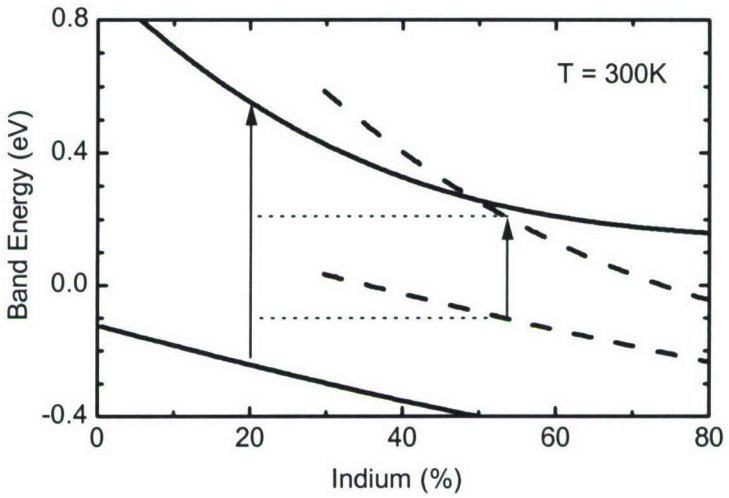

Figure 2.3. Conduction and valence band positions vs. indium concentration for quinternary InAlGaAsSb waveguide lattice matched to GaSb (solid lines) and 1.8 % strained quaternary InGaAsSb QW composition (dashed lines). Vertical arrows indicate bulk-like energy gaps for waveguide/QW compositions corresponding to the laser design described in the text.

The vertical arrow on the left indicate the direct energy gaps for quinternary waveguide with 20 % Al and 20 % In. The right arrow corresponds to a 1.8 % strained quaternary QW with 54 % In. Alternatively, the heterobarrier height for holes in the QW heterostructure with AlGaAsSb waveguide can be improved with increase of the Al composition (see Figures 2.1 and 2.2) however this approach is less desirable since it reduces the waveguide refractive index and, consequently, compromises the optical confinement.

Figure 2.4 shows the temperature dependence of CW light-current characteristics for 2-mm-long devices fabricated with quinternary AlInGaAsSb waveguide. A higher CW output power in excess of 130 mW and a lower threshold current of 0.6 A at T= 290 K were demonstrated in comparison to results obtained with quaternary AlGaAsSb barriers.

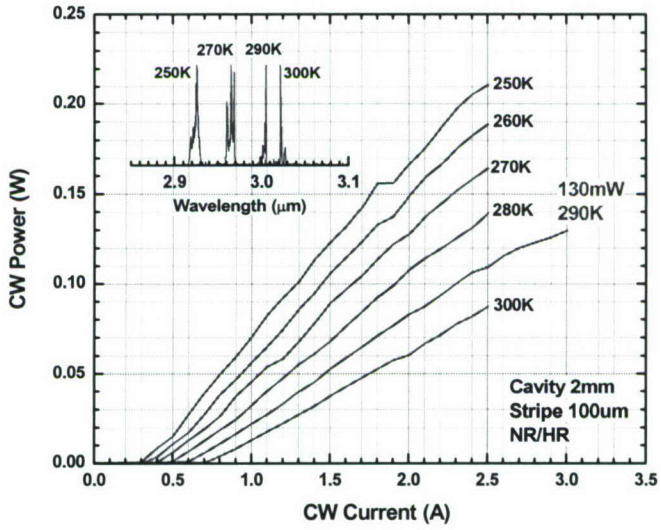

Figure 2.4. Temperature dependence of CW light-current characteristics of the GaSb-based lasers emitting at 3μm at room temperature. Insert shows laser spectra near threshold.

The data presented above demonstrate that InGaAsSb laser heterostructures with quinternary InAlGaAsSb waveguide are promising for fabrication of GaSb-based type-I diode lasers with emission wavelengths above 3 μm. Structures with quaternary AlGaAsSb waveguides/barriers have limitations which restrict their use for device development in this spectral range.

3. Direct measurements of the interband optical absorption in laser structures with type-I and type-II band alignments. Temperature sensitivity of the threshold current in type-I and type-II mid-infrared semiconductor lasers. (in collaboration with Albuquerque Air Force Research Laboratory)

Drect measurements of the interband optical absorption in laser structures with type-I and type-II band alignments showed that the difference in the optical matrix elements is insignificant for these two groups of structures. We show that thermally-induced hole escape from the active quantum wells strongly deteriorates the optical emission in both types of heterostructures. Experiments show that the temperature decay of PL is stronger in type-II heterostructures then in type-I ones with the same hole confinement energies.

We study two groups of samples with predominantly type I and type II band alignment. Each group consists of two structures which are characterized by different hole confinement. The maximum absorption per quantum well in the type I structure was only about 50% higher than in type II structure (Figure 3.1). We, therefore, rule out the reduced optical gain as a mechanism for the inferior temperature performance of type II mid-IR lasers.

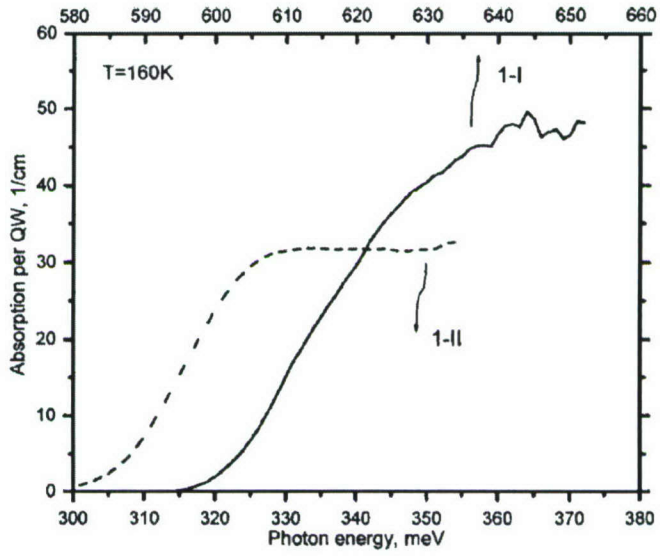

Figure 3.1. Optical absorption per quantum well for type-II samples (dashed line) and type-I ones (solid line).

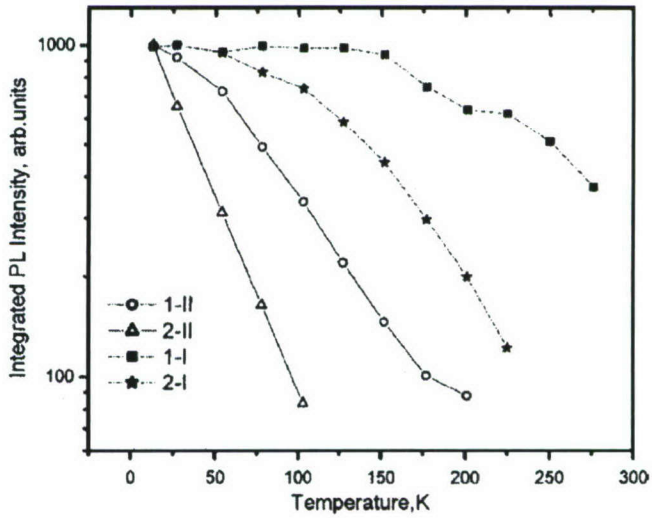

Figure 3.2. Integrated PL intensity versus temperature for type-II (solid lines) and type-I (dashed lines) heterostructures. Samples denoted as 1-II and 1-I have strong hole confinement and samples 2-II and 2-I have pour hole confinement.

To study the recombination in type I and type II structures, we measured the integrated PL intensity as a function of temperature (Figure 3.2). For convenience, all the curves are normalized to the lowest-temperature value. The high temperature decay of the PL is due to thermal depopulation of the quantum wells. The strength of the PL temperature quenching in

each group of structures correlates well with the degree of the hole confinement. The nature of the observed difference in temperature dependencies of photoluminescence for type I and type II structures is not fully understood. One of the possibilities is an excessive nonradiative carrier losses which can be associated with interface assisted recombination in narrow QWs.

4. Carrier capture and hole localization in type-II QW optically pumped lasers. (in collaboration with Albuquerque Air Force Research Laboratory)

We performed direct measurements of the carrier capture in GaSb-based type-II QWs. Three structures were studied: W-QW with both electron and hole confinement QWs, InAs QW with electron confinement only (same electron QW as in W-QW design) and InGaSb QW with hole confinement only (same hole QW like in W-QW design). The carrier capture was characterized by measuring temporal decay of the photoluminescence from InGaAsSb barrier layers. Figure 4.1a shows that barrier layer PL decays measured for structures with W and InAs electron QWs are fast and on tens of picosecond scale. The corresponding PL decay measured for structures with InGaSb hole QWs is on nanosecond scale and, thus, determined by carrier lifetime in InGaAsSb barrier layer. Temperature dependence of the PL spectra supports this conclusion since at high temperatures the PL from InGaSb disappears while PL from InGaAsSb barrier layer is present (Figure 4.1b). This is direct evidence that at higher temperatures most of the holes in W-QW lasers are delocalized from QW and mainly in barrier layer due to its higher density of states. This hole delocalization decreases device differential gain at high temperatures contributing to pour room temperature performance of the type-II QW lasers with present design.

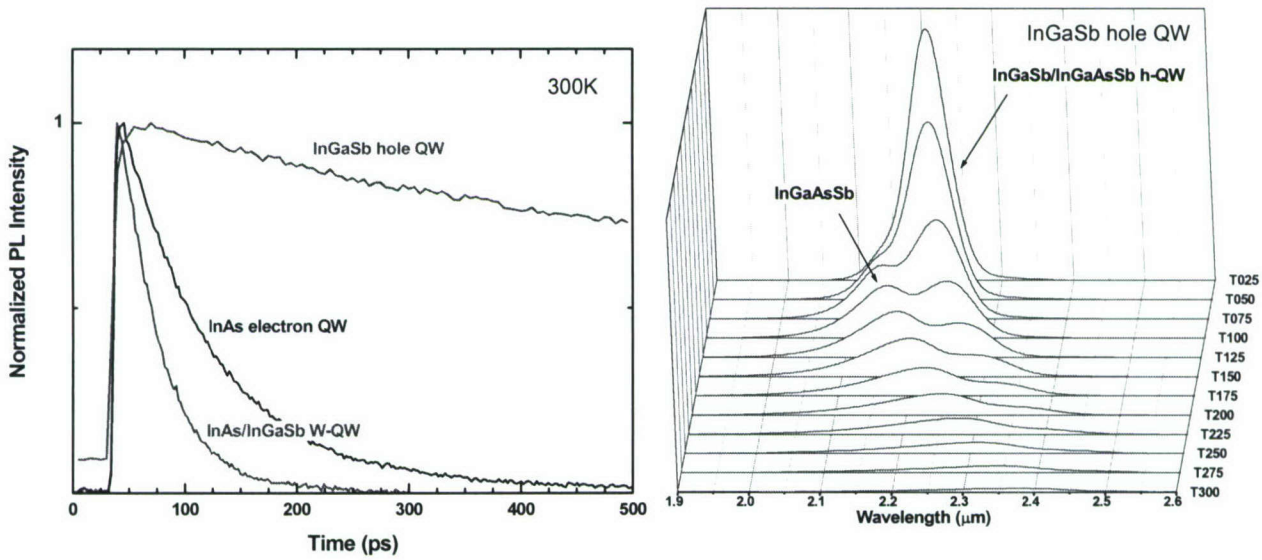

Figure 4.1. Decay of the photoluminescence from the barrier layer (a) and temperature dependence of the PL spectra from heterostructure with InGaSb hole QW (b).

5. Dilute-nitride materials for mid-infrared emitters and detectors. (in collaboration with Army Research Laboratory).

MBE growth of the GaSbN dilute-nitride material on GaSb substrates was performed. X-ray measurements indicate incorporation of the nitrogen into the lattice. Optical absorption, low temperature equilibrium photoluminescence as well as ultra-fast photoluminescence up-conversion experiments conclusively indicate formation of the nitrogen related states with energy below band gap of GaSb material.

Sample (K0-544) with GaSbN bulk region of total thickness of about 1μm was grown by solid-source MBE at Army Research Lab. Thin AlSb cladding layers were implemented on both sides of the dilute-nitride layer to confine carriers in layer or interest for photoluminescence (PL) studies. The nitrogen composition was kept low (0.28%) to minimize problems with dislocation formation. A reference sample was also grown without N but under otherwise identical conditions (K0543). X-ray diffraction was done at ARL and the samples were sent to SUNY.
The absorption of ARL samples K0543-4 was first studied in a test geometry as shown in Figure 5.1

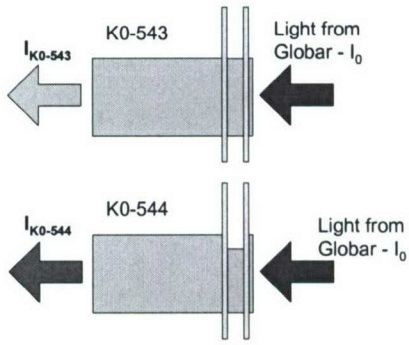

Figure 5.1. Optical transmission experiment

A slight difference in the absorption was seen as demonstrated in Figure 5.2a and further enhanced by plotting the logarithm of the difference in Figure 5.2b.

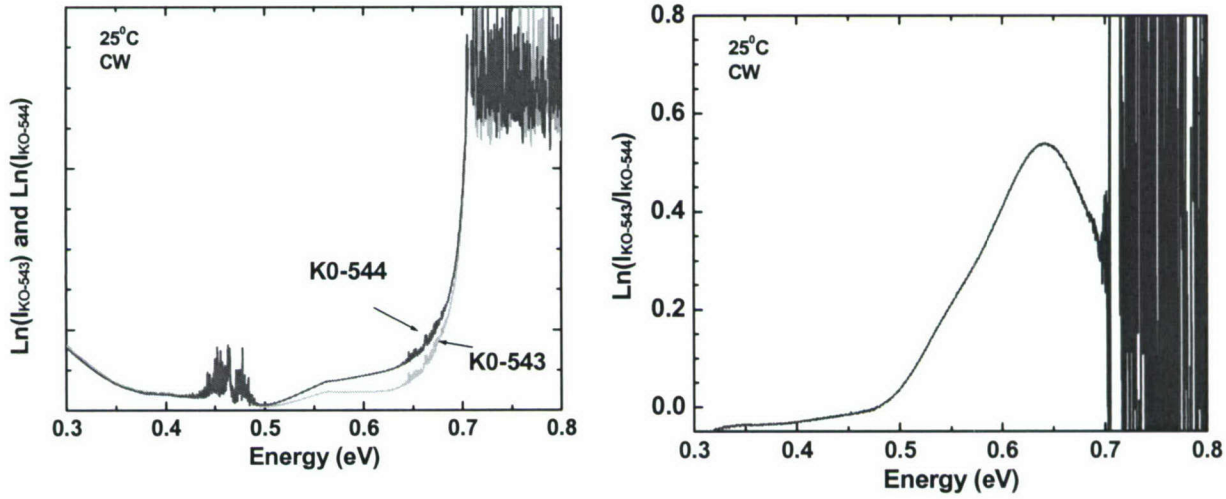

Figure 5.2. (a) RT transmission from $GaSbN_X$ samples with x=0.28% (magenta) and x=0% (blue). (b) shows the logarithm of the difference intensities highlighting absorption below the GaSb bandgap.

Next the sample's carrier relaxation dynamics were studied with an ultra-fast photoluminescence up-conversion–method capable of detecting the PL from materials with very short carrier lifetimes. The results are shown in Figure 5.3 and demonstrate the presence of a very fast recombination center(s) in the sample with nitrogen.

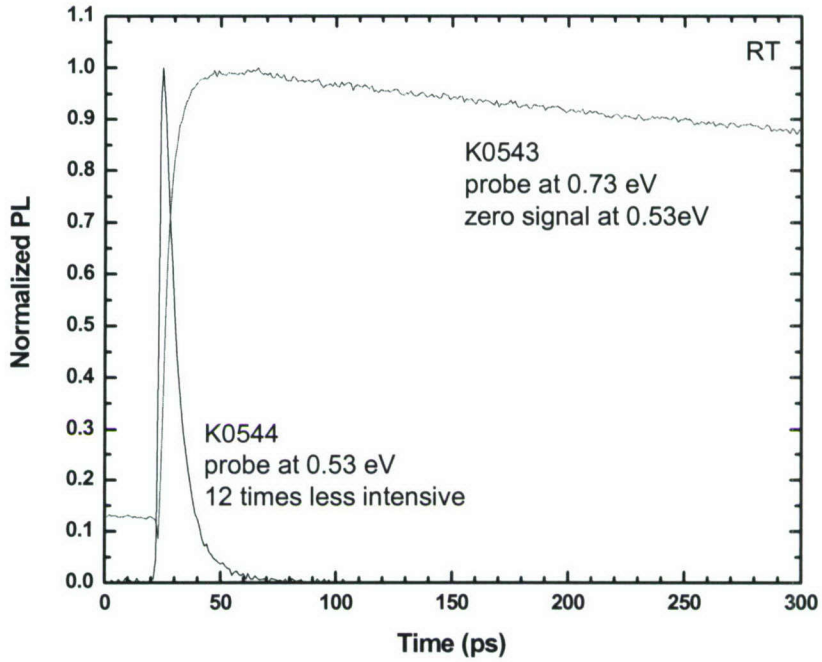

Figure 5.3. Ultra fast RT PL. Presence of the fast recombination centers at 0.53eV only in K0544 correlates with absorption data

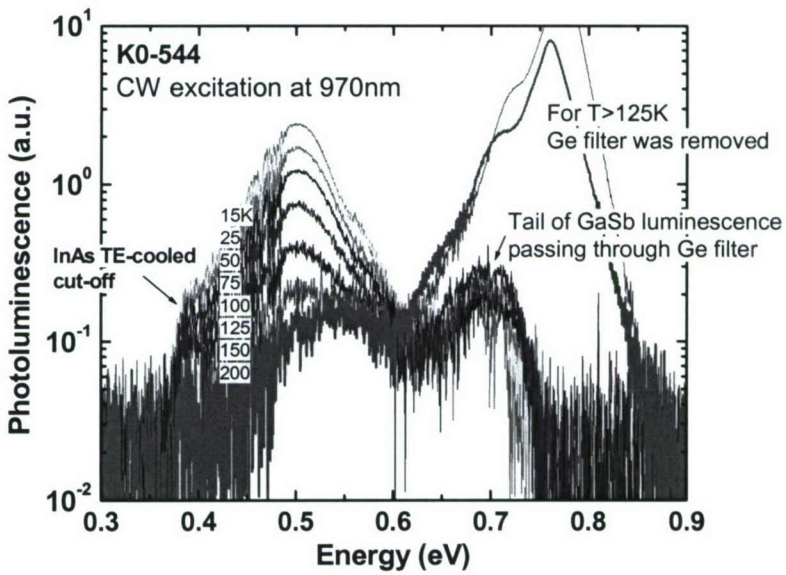

Figure 5.4. Sample temperature evolution of CW PL from the GaSbN sample.

Finally, CW PL studies were performed at low temperatures (Figure 5.4). A feature centered around 0.5 eV was clearly seen in the nitrogen-containing sample and was studied as a function of temperature. At present its origin is not clear.

Summary and further outlook.

We report on record-breaking output performance from new electrically powered semiconductor lasers emitting in the mid-infrared spectral region at wavelengths of 3.0 and 3.1 micrometers. The devices operate at room temperature and produce continuous output powers up to 32 times higher than devices previously reported.

Devices designed with barrier layers consisting of the quaternary alloy AlGaAsSb and emitting at 3.1μm demonstrated a continuous output power of 80mW at room temperature. Devices designed with quinternary AlInGaAsSb barrier layers produced a continuous 130mW of 3μm optical power at room temperature. Room temperatures pulsed power outputs of 750mW at 3.1 micrometers and over 1W at 3.0 micrometers were observed.

Importance of proper hole confinement in GaSb-based photonic nanostructures was identified by set of specially designed experimental studies and by theoretical modeling. Record 17.5% power conversion efficiency was obtained from CW room temperature operated diode lasers putting out above 1W in spectral region 2.3-2.4μm.

Project findings have defined the design approach for fabrication of the new class diode lasers for spectral region from 3 to 3.5μm. Combination of the compressively strained QW active region with novel quinternary barrier material will allow for fabrication of the watt class lasers and mW class light emitting diodes with improved power-conversion efficiency and operating at room temperature in CW regime.

Supported Personnel

G.L. Belenky	Professor/Distinguished Professor
L. Shterengas	Postdoctoral Associate/Research Scientist/Assistant Professor
M. Kisin	Senior Scientist
G. Kipshidze	Senior Scientist
A. Gourevitch	Ph.D. Student
T. Hosoda	PhD student
J. Seung Yong	PhD student

Dissertations

The work performed under the sponsorship of this project constitutes significant part of the PhD dissertation of Dr. Gourevitch "Design and characterization of InGaAsP/InP and In(Al)GaAsSb/GaSb laser diode arrays", SUNY at Stony Brook 2006.
PhD dissertations of the Mr. Hosoda and Mr. J. Seung Yong (estimated graduation year 2011) will include the work performed in the framework of the current project.

Publications

Journal papers

1. L. Shterengas, G. Belenky, J.-Y. Yeh, L.J. Mawst, N. Tansu, "Differential gain and linewidth-enhancement factor in dilute-nitride GaAs-based 1.3μm diode lasers", J. Sel. Top. Quantum Electron. 11, 1063 (2005).

2. A. Thränhardt, I. Kuznetsova, C. Schlichenmaier, S. W. Koch, L. Shterengas, G. Belenky, J.-Y. Yeh, L. J. Mawst, N. Tansu, J. Hader, J.V. Moloney, and W.W. Chow, "Nitrogen incorporation effects on gain properties of GaInNAs lasers: Experiment and theory", Appl. Phys. Lett. 86, 201117 (2005).

3. P.J. McCann, P. Kamat, Y. Li, A. Sow, H.Z. Wu, G. Belenky, L. Shterengas, J.G. Kim, R. Martinelli, "Optical pumping of IV-VI semiconductor multiple quantum well materials using a GaSb-based laser with emission at λ=2.5μm", J. Appl. Phys. 97, 053103 (2005)

4. S. Suchalkin, L. Shterengas, M. Kisin, S. Luryi, G. Belenky, R. Kaspi, A. Ongstad, J.G. Kim, R.U. Martinelli, "Mechanism of the temperature sensitivity of mid-IR GaSb based semiconductor lasers", Appl. Phys. Lett. 87, 041102 (2005).

5. L. Shterengas, R. Kaspi, A. Ongstad, S. Suchalkin, G. Belenky, "Carrier capture in InGaAsSb/InAs/InGaSb type-II laser heterostructures", Appl. Phys. Lett. 91, 101106 (2007).

6. D. Donetsky, G. Kipshidze, L. Shterengas, T. Hosoda, and G. Belenky, "2.3 μm type-I quantum well GaInAsSb/AlGaAsSb/GaSb laser diodes with quasi-CW output power of 1.4 W", Electron. Lett. 43 (15), 810-812 (2007).

7. L. Shterengas, G. Belenky, M. Kisin, D. Donetsky, "High power 2.4μm heavily strained Type-I QW GaSb-based diode lasers with above 1W CW output and power conversion efficiency of 17.5%", Appl. Phys. Lett. 90, 011119 (2007).

8. G. Belenky, D. Donetsky, L. Shterengas, T. Hosoda, J. Chen, G. Kipshidze, M. Kisin, D. Westerfeld, "Interband GaSb-based laser diodes for spectral regions of 2.3-2.4μm and 3-3.1μm with improved room-temperature performance", accepted to SPIE Proceedings.

9. T. Hosoda, G. Belenky, L. Shterengas, G. Kipshidze, M.V. Kisin, "Continuous-wave room temperature operated 3.0μm Type I GaSb-based lasers with quinternary AlInGaAsSb barriers", accepted to Appl. Phys. Lett.

10. D. Donetsky, J. Chen, L. Shterengas, G. Kipshidze, D. Westerfeld, "2.3μm high-power Type-I quantum-well GaInAsSb/AlGaAsSb/GaSb laser diode arrays with an increased fill-factor", submitted to J. Electron. Mat.

11. L. Shterengas, G. Belenky, G. Kipshidze, T. Hosoda, "Room temperature operated 3.1-μm type-I GaSb-based diode lasers with 80mW continuous wave output power", to be submitted to IEEE Photon. Technol. Lett.

Invited conference presentations

1. G.L. Belenky, L. Shterengas, J.G. Kim, R. Martinelli, S. Suchalkin, M.V. Kisin, "GaSb-based lasers for spectra region 2-4μm: challenges and limitations," Photonics West, January 24-29 (2005), San Jose, California, USA, Proc. SPIE Int. Soc. Opt. Eng. 5732 (2005) 169.

2. J. G. Kim, H. An, L. Shterengas, R. U. Martinelli, G. L. Belenky, "Development of high-power room-temperature continuous wave operation of 2.0-2.8um type-I In(Al)GaAsSb/GaSb diode lasers," The 2nd Symposium on Infrared Materials and Technologies, November 21 – 22 (2005), The Penn State Conference Center Hotel, State College, Pennsylvania, USA.

3. G. Belenky, S. Suchalkin, S. Luryi, L. Shterengas, J. Bruno, R. Tober, R.U. Martinelli, J.G. Kim, "2μm – 5μm GaSb based emitters for free space communications. Challenges and limitations", SPIE International Symposium "Information Technology and Communication", October 25-28 (2004), Philadelphia, Pennsylvania, USA.

4. L. Shterengas, G. Kipshidze, G. Belenky, "Room temperature operated type-I QW GaSb-based light emitters with wavelength up to 3.4μm," The 13th International Conference on Narrow Gap Semiconductors, July 9-12 (2007), University of Surrey, Guildford, Surrey, UK.

5. G. Belenky, L. Shterengas, S. Suchalkin, G. Kipshidze, M. Kisin, D. Donetsky, "Interband GaSb-based lasers and LED for spectral region above 2μm", SPIE Photonics West, 19-24 January (2008), San Jose, California, USA.

Conference presentations

1. G.L. Belenky, J.G. Kim, L. Shterengas, R.U. Martinelli, "Mid-IR room temperature operated GaSb-based lasers and laser arrays," 17th Annual Meeting of the IEEE Laser and Electro-Optics Society, November 7—11 (2004), Puerto Rico, Proc. v.2 p.553.

2. L. Shterengas, J.-Y. Yeh, L.J. Mawst, N. Tansu, G. Belenky, "Linewidth-enhancement factors of InGaAs and InGaAsN single-quantum-well diode lasers", Conference on Lasers and Electro-Optics, May 16-21 (2004) San Francisco, California.

3. L. Shterengas, G. Belenky, J.G. Kim, A. Gourevitch, D. Donetsky, D. Westerfeld, R. Martinelli, "Effect of compressive strain on differential gain of GaSb-based type-I QW lasers," Conference on Lasers and Electro-Optics, May 21-26 (2006) Long Beach, California, USA.

4. L. Shterengas, A. Ongstad, R. Kaspi, S. Suchalkin, G. Belenky, M. Kisin, D. Donetsky, "Carrier Capture in InGaAsSb/InAs/InGaSb Type-II QW Laser Heterostructures," Conference on Lasers and Electro-Optics, May 21-26 (2006) Long Beach, California, USA.

5. D. Donetsky, L. Shterengas, G. Kim, G. Belenky, A. Gourevitch, D. Westerfeld, R. Martinelli, "Carrier Recombination Kinetics in 2.3-2.4 μm InGaAsSb/AlGaAsSb QW Laser Heterostructures", Electronic Materials Conference, June 28-30 (2006) Pennsylvania State University, Pennsylvania, USA.

6. L. Shterengas, A. Ongstad, R. Kaspi, S. Suchalkin, G. Belenky, M. Kisin, D. Donetsky, "Electron and Hole Energy Relaxation in InGaAsSb/InAs/InGaSb Type-II QW Laser Heterostructures", Electronic Materials Conference, June 28-30 (2006) Pennsylvania State University, Pennsylvania, USA.

7. M. V. Kisin, L. Shterengas, J.G. Kim, G. Belenky, "Enhancement of Optical Gain in Sb-based MIR Diode Lasers", International Semiconductor Laser Conference, September 18-21 (2006), Kohala Coast, Hawaii, USA.

8. L. Shterengas, D. Donetsky, M. Kisin, G. Belenky, "Carrier capture and recombination in 2.4μm GaSb-based type-I quantum well high power diode lasers", Conference on Lasers and Electro-Optics, May 6-11 (2007) Baltimore, Maryland, USA.

9. L. Shterengas; G. Belenky; M. Kisin; D. Donetsky; D. Westerfeld, "Recent developments in high power 2.3-2.4μm diode lasers", SPIE, 6552, 655214, Laser Source Technology for Defense and Security III (2007).

10. J. G. Kim, H. An, L. Shterengas, R. U. Martinelli, G. L. Belenky, "Development of high-power room-temperature continuous wave operation of 2.0-2.8μm type-I In(Al)GaAsSb/GaSb diode lasers," The 2nd Symposium on Infrared Materials and Technologies, November 21 – 22 (2005), The Penn State Conference Center Hotel, State College, Pennsylvania, USA.